This is a repository copy of *Directional modulation design under a constant magnitude constraint for weight coefficients*.

White Rose Research Online URL for this paper:
http://eprints.whiterose.ac.uk/152870/

Version: Published Version

Directional Modulation Design Under a Constant Magnitude Constraint for Weight Coefficients

BO ZHANG[ID]1, (Member, IEEE), **WEI LIU**[ID]2, (Senior Member, IEEE),
YANG LI[ID]1, **XIAONAN ZHAO**[ID]1, **AND CHENG WANG**[ID]1
[1]Tianjin Key Laboratory of Wireless Mobile Communications and Power Transmission, College of Electronic and Communication Engineering, Tianjin Normal University, Tianjin 300387, China
[2]Communications Research Group, Department of Electronic and Electrical Engineering, The University of Sheffield, Sheffield S1 4ET, U.K.

Corresponding author: Bo Zhang (b.zhangintj@tjnu.edu.cn)

ABSTRACT Directional modulation (DM) as a physical layer security technique has been studied from many different aspects recently. Normally all existing designs based on antenna arrays lead to varying weight coefficients for different antennas and for different signal symbols, which poses a particular challenge for feed circuits design in analogue implementation. In this paper, to reduce the implementation complexity, a constant magnitude constraint is proposed for the first time, and the resultant non-convex constraint can be modified to a convex form so that the problem can be solved conveniently by existing convex optimisation toolboxes. Design examples are provided to show the effectiveness of the proposed design.

INDEX TERMS Constant magnitude constraint, directional modulation, linear antenna array.

I. INTRODUCTION

With the fast development of the Fifth Generation (5G) network, communication has been more important than ever [1], [2]. As physical layer security technique to keep known constellation mappings in a desired direction or directions, while scrambling them for the remaining ones, directional modulation (DM) has been studied widely [3]. In [4], a four-element reconfigurable antenna array was designed, where the DM design was achieved by changing elements for each symbol. In [5], phased antenna array was employed for DM, with an individual tailor-made feed circuit (including phase shift and amplitude change) prepared for each antenna. Compared with a given antenna array design, to further reduce the number of antennas, DM design was extended to sparse antenna arrays [6]. To overcome the inherent limitation of DM, where eavesdroppers and the desired users share the same received signal when they are in the same spatial direction of the antenna array, two positional modulation (PD) designs were proposed, with one based on a reflecting surface [7], and the other employing multiple antenna arrays [8]. Both designs are based on the idea that if the received signal is a combination of signals from different

paths with different directions, then signals at these locations can be distinguished. To increase the channel capacity of DM, two antenna array structures were proposed recently. One uses a crossed-dipole antenna array [9], where two DM signals with orthogonal polarisations are transmitted in the same direction. The second one employs multiple frequencies, leading to an orthogonal frequency division multiplexing (OFDM) type structure based on the inverse Discrete Fourier Transform (IDFT) [10], [11]. A method named dual beam DM was introduced in [12]. Different from the traditional design where inphase and quadrature (IQ) components of signals are transmitted by the same antenna, dual beam DM design transmits these two components by different antennas. In [13], directional antennas were used in the design instead of isotropic antennas, and a narrower low BER range was achieved. In [14], the BER was employed for DM transmitter synthesis by linking the BER performance to the settings of phase shifters. A pattern synthesis approach was presented in [15], [16], where information pattern and interference patterns are created together to achieve DM, followed by an eight-element time-modulated antenna array in [17], an artificial-noise-aided zero-forcing synthesis approach in [18], and a multi-relay design in [19].

Recently, the introduction of artificial noise (AN) has further advanced the directional modulation technology. AN can

The associate editor coordinating the review of this manuscript and approving it for publication was Qilian Liang[ID].

be categorised into 'static' AN and 'dynamic' AN. Static AN results in scrambled but fixed constellation points in undesired directions, while dynamic AN keeps the scrambled points change with time. For the construction of AN, two methods were introduced. One is the orthogonal vector method [20], [21], where the added AN vector is orthogonal to the steering vector of the desired direction. The other one is the AN projection matrix method [22], [23], where by designing an artificial noise projection matrix, the AN vector is projected into the zero space of the derivative of the desired direction.

However, the resultant weight coefficients for existing DM designs vary with different antennas, in particular in their magnitudes. When implemented by analogue circuits, both magnitude and phase responses of the feed circuits will be different for different antennas and different symbols, which will increase the implementation complexity of the whole system. To reduce this complexity, in this paper, a constant magnitude constraint is proposed for the DM design, and the resultant non-convex optimization problem is then transformed into a convex one to facilitate its solution. In general, the resultant weight coefficient magnitude is the same for all antennas for the same symbol. When all the symbols have the same magnitude, such as in phase shift keying (PSK) modulation, the weight coefficient magnitude will be the same for all antennas and symbols, further reducing the implementation complexity of the whole system.

The remaining part of this paper is structured as follows. A review of DM design based on narrowband linear antenna arrays is given in Sec. II. The constant magnitude constraint for weight coefficients is introduced and a solution to the constrained design problem is derived in Sec. III. In Sec. IV, design examples are provided, with conclusions drawn in Sec. V.

II. REVIEW OF DM DESIGN BASED ON NARROWBAND LINEAR ANTENNA ARRAYS

A. NARROWBAND BEAMFORMING

A narrowband linear antenna array for transmit beamforming is shown in Fig. 1, which has N omni-directional antennas with the corresponding weight coefficient w_n ($n = 0, 1, \ldots, N-1$) and spacing d_n for $n = 1, \ldots, N-1$ between the first antenna to its subsequent antennas. The spatial angle $\theta \in [0°, 180°]$. The steering vector of the array as a function of angular frequency ω and spatial angle θ, is given by

$$\mathbf{s}(\omega, \theta) = [1, e^{j\omega d_1 \cos\theta/c}, \ldots, e^{j\omega d_{N-1} \cos\theta/c}]^T, \quad (1)$$

where $\{\cdot\}^T$ is the transpose operation, and c is the speed of propagation. For a uniform linear array (ULA) with a half-wavelength spacing ($d_n - d_{n-1} = \lambda/2$) between adjacent antennas, the steering vector can be simplified to

$$\mathbf{s}(\omega, \theta) = [1, e^{j\pi \cos\theta}, \ldots, e^{j\pi(N-1)\cos\theta}]^T. \quad (2)$$

The corresponding weight coefficients can be put together as a vector $\mathbf{w}$,

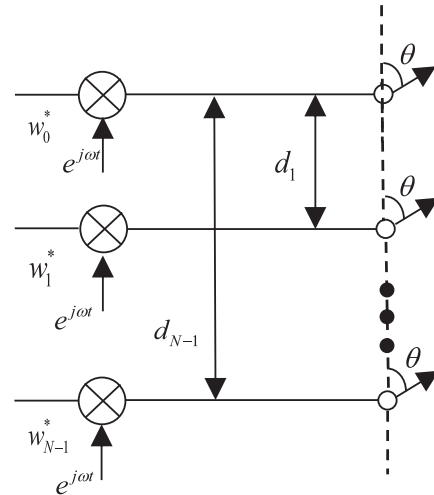$$\mathbf{w} = [w_0, w_1, \ldots, w_{N-1}]^T. \quad (3)$$

FIGURE 1. A narrowband transmit beamforming structure.

Then, the beam response of the array can be given by

$$p(\omega, \theta) = \mathbf{w}^H \mathbf{s}(\omega, \theta), \quad (4)$$

where $\{\cdot\}^H$ represents the Hermitian transpose.

B. DM DESIGN BASED ON THE ABOVE STRUCTURE

The aim of DM design is to keep known constellation mappings in a desired direction or directions, while scrambling them for the remaining ones. To achieve it, we need to find the corresponding sets of weight coefficients for all symbols. Here, for M-ary signaling, such as multiple phase shift keying (MPSK), there are M sets of desired array responses $p_m(\theta)$, with the corresponding weight vector

$$\mathbf{w}_m = [w_{m,0}, w_{m,1}, \ldots, w_{m,N-1}]^T, \quad m = 0, 1, \ldots, M-1. \quad (5)$$

Each desired response $p_m(\omega, \theta)$ can be classified into one of the two regions: the mainlobe response $\mathbf{p}_{m,ML}$, and the sidelobe response $\mathbf{p}_{m,SL}$. Here we assume r points $\theta_0, \theta_1, \ldots, \theta_{r-1}$ are sampled in the mainlobe, and $R-r$ points $\theta_r, \theta_{r+1}, \ldots, \theta_{R-1}$ in the sidelobe. Then, the desired beam responses in the mainlobe and sidelobe regions for the m-th symbol can be represented by

$$\mathbf{p}_{m,ML} = [p_m(\omega, \theta_0), p_m(\omega, \theta_1), \ldots, p_m(\omega, \theta_{r-1})],$$
$$\mathbf{p}_{m,SL} = [p_m(\omega, \theta_r), p_m(\omega, \theta_{r+1}), \ldots, p_m(\omega, \theta_{R-1})]. \quad (6)$$

Similarly, the steering matrix for mainlobe and sidelobe ranges can be expressed as

$$\mathbf{S}_{ML} = [\mathbf{s}(\omega, \theta_0), \mathbf{s}(\omega, \theta_1), \ldots, \mathbf{s}(\omega, \theta_{r-1})],$$
$$\mathbf{S}_{SL} = [\mathbf{s}(\omega, \theta_r), \mathbf{s}(\omega, \theta_{r+1}), \ldots, \mathbf{s}(\omega, \theta_{R-1})]. \quad (7)$$

Note that all symbols for a fixed θ share the same steering vector.

Based on the above parameters, for the m-th symbol, its corresponding weight coefficients for DM design can be

TABLE 1. Mainlobe and sidelobe regions.

Mainlobe region:	$\theta_0, \theta_1, \ldots, \theta_{r-1}$
Sidelobe region:	$\theta_r, \theta_{r+1}, \ldots, \theta_{R-1}$

obtained by solving the following problem

$$\min ||\mathbf{p}_{m,SL} - \mathbf{w}_m^H \mathbf{S}_{SL}||_2$$
$$\text{subject to } \mathbf{w}_m^H \mathbf{S}_{ML} = \mathbf{p}_{m,ML}, \qquad (8)$$

where $|| \cdot ||_2$ denotes the l_2 norm. The cost function is to minimise the difference between desired and designed sidelobe responses, and the equality constraint is to make sure the main lobe direction has the desired symbol response.

III. CONSTANT MAGNITUDE CONSTRAINT FOR WEIGHT COEFFICIENT

However, the magnitudes of weight coefficients in (8) are not the same for different antennas and different symbols. In other words, we need an individual tailor-made feed circuit (including phase shift and amplitude change) for each antenna for analogue implementation. To simplify implementation of a DM design, in this section, we introduce a constant magnitude constraint for weight coefficients, i.e.,

$$|w_{m,n}| = \delta_m, \quad n = 0, 1, \ldots, N - 1, \qquad (9)$$

where δ_m represents the given magnitude for each weight coefficient for the m-th symbol, so that we only need to change the phase response of the feed circuit for different antennas. The mainlobe and sidelobe regions are shown in Table 1. The DM design under the constant magnitude constraint for weight coefficient can be formulated as follows

$$\min ||\mathbf{p}_{m,SL} - \mathbf{w}_m^H \mathbf{S}_{SL}||_2$$
$$\text{subject to } \mathbf{w}_m^H \mathbf{S}_{ML} = \mathbf{p}_{m,ML}$$
$$|w_{m,n}| = \delta_m$$
$$n = 0, 1, \ldots, N - 1. \qquad (10)$$

However, δ_m is not arbitrary, and there is a valid range for it. To derive it, we first have

$$\mathbf{w}_m^H \mathbf{s}(\omega, \theta_{\hat{r}})$$
$$= p_m(\omega, \theta_{\hat{r}})$$
$$\Rightarrow |\mathbf{w}_m^H \mathbf{s}(\omega, \theta_{\hat{r}})| = |p_m(\omega, \theta_{\hat{r}})|$$
$$= |w_{m,0}^* + w_{m,1}^* e^{j\omega d_1 \cos\theta_{\hat{r}}/c} + \ldots + w_{m,N-1}^* e^{j\omega d_{N-1} \cos\theta_{\hat{r}}/c}|$$
$$\leq |w_{m,0}^*| + |w_{m,1}^* e^{j\omega d_1 \cos\theta_{\hat{r}}/c}| + \ldots$$
$$\quad + |w_{m,N-1}^* e^{j\omega d_{N-1} \cos\theta_{\hat{r}}/c}|$$
$$\leq |w_{m,0}^*| + |w_{m,1}^*| \cdot |e^{j\omega d_1 \cos\theta_{\hat{r}}/c}| + \ldots$$
$$\quad + |w_{m,N-1}^*| \cdot |e^{j\omega d_{N-1} \cos\theta_{\hat{r}}/c}|$$
$$\leq |w_{m,0}^*| + |w_{m,1}^*| + \ldots + |w_{m,N-1}^*|, \qquad (11)$$

for $\hat{r} = 0, 1, \ldots, R - 1$ including mainlobe and sidelobe regions.

Due to the proposed constant magnitude constraint, where the magnitudes of all weight coefficients have to be the same, i.e.,

$$|w_{m,0}^*| = |w_{m,1}^*| = \ldots = |w_{m,N-1}^*|, \qquad (12)$$

(11) can be further simplified to

$$|p_m(\omega, \theta_{\hat{r}})| \leq N|w_{m,n}^*| = N|w_{m,n}|. \qquad (13)$$

Therefore, we have

$$|w_{m,n}| \geq \frac{|p_m(\omega, \theta_{\hat{r}})|}{N}. \qquad (14)$$

Since the maximum value of $\frac{|p_m(\omega, \theta_{\hat{r}})|}{N}$ is

$$\max \left(\frac{|p_m(\omega, \theta_{\hat{r}})|}{N} \right) = \frac{|p_m(\omega, \theta_0)|}{N}, \qquad (15)$$

where θ_0 represents the mainlobe direction with the maximum magnitude response value, we have

$$|w_{m,n}| \geq \frac{|p_m(\omega, \theta_0)|}{N}. \qquad (16)$$

Then, with the equality constraint $|w_{m,n}| = \delta_m$ for $n = 0, 1, \ldots, N - 1$ from (10), the inequality (16) can be replaced by

$$|w_{m,n}| = \delta_m$$
$$\delta_m \geq \frac{|p_m(\omega, \theta_0)|}{N}. \qquad (17)$$

Then, the formulation in (10) becomes

$$\min ||\mathbf{p}_{m,SL} - \mathbf{w}_m^H \mathbf{S}_{SL}||_2$$
$$\text{subject to } \mathbf{w}_m^H \mathbf{S}_{ML} = \mathbf{p}_{m,ML}$$
$$\delta_m \geq \frac{|p_m(\omega, \theta_0)|}{N}$$
$$|w_{m,n}| = \delta_m$$
$$n = 0, 1, \ldots, N - 1. \qquad (18)$$

For the purpose of saving the transmission power for each antenna, i.e., setting the minimum magnitude of weight coefficient, we select the minimum value of the constant magnitude

$$\delta_m = \frac{|p_m(\omega, \theta_0)|}{N}. \qquad (19)$$

Note that in practice if we need to increase the transmission power of the array to increase its communication range, we can uniformly increase the magnitude of all coefficients accordingly. Therefore, using (19) to set the minimum transmission power will not cause any additional issues in practice. Then, the formulation (18) becomes

$$\min ||\mathbf{p}_{m,SL} - \mathbf{w}_m^H \mathbf{S}_{SL}||_2$$
$$\text{subject to } \mathbf{w}_m^H \mathbf{S}_{ML} = \mathbf{p}_{m,ML}$$
$$|w_{m,n}| = \frac{|p_m(\omega, \theta_0)|}{N}$$
$$n = 0, 1, \ldots, N - 1. \qquad (20)$$

Note that for the above formulation to work, the maximum magnitude response in the mainlobe can only be located at one single direction (θ_0 in our case), i.e., a flat top main beam can not be achieved. We will prove this later at the end of Section III. Here, with the single maximum mainlobe direction represented by θ_0, the formulation (20) can be simplified to

$$
\min \ ||\mathbf{p}_{m,SL} - \mathbf{w}_m^H \mathbf{S}_{SL}||_2
$$
$$
\text{subject to } \mathbf{w}_m^H \mathbf{s}(\omega, \theta_0) = p_m(\omega, \theta_0)
$$
$$
|w_{m,n}| = \frac{|p_m(\omega, \theta_0)|}{N}
$$
$$
n = 0, 1, \ldots, N-1. \tag{21}
$$

Moreover, the equality constraint $|w_{m,n}| = \frac{|p_m(\omega,\theta_0)|}{N}$ in (21) is non-convex. To solve the problem using the CVX toolbox in Matlab, we propose a new constraint

$$
||\mathbf{w}_m||_\infty \leq \frac{|p_m(\omega, \theta_0)|}{N}, \tag{22}
$$

to replace the equality constraint $|w_{m,n}| = \frac{|p_m(\omega,\theta_0)|}{N}$ in (21), where $|| \cdot ||_\infty$ represents the l_∞ norm (the maximum magnitude of the entries in the vector). This inequality constraint is to set the entry with the maximum magnitude of the vector $\mathbf{w}_m$ no greater than $\frac{|p_m(\omega,\theta_0)|}{N}$. According to (16), if the maximum value or any other entries of the vector is less than $\frac{|p_m(\omega,\theta_0)|}{N}$, then the constraint $\mathbf{w}_m^H \mathbf{s}(\omega, \theta_0) = p_m(\omega, \theta_0)$ cannot be satisfied. Therefore, the proposed constraint (22) can force all entries of the vector to have the same value as $\frac{|p_m(\omega,\theta_0)|}{N}$.

Then, the DM design under the constant magnitude constraint can be modified into

$$
\min \ ||\mathbf{p}_{m,SL} - \mathbf{w}_m^H \mathbf{S}_{SL}||_2
$$
$$
\text{subject to } \mathbf{w}_m^H \mathbf{s}(\omega, \theta_0) = p_m(\omega, \theta_0)
$$
$$
||\mathbf{w}_m||_\infty \leq \frac{|p_m(\omega, \theta_0)|}{N}. \tag{23}
$$

The above problem (23) can be solved by the CVX toolbox in MATLAB [24], [25].

Note that if

$$
|p_0(\omega, \theta_0)| = |p_m(\omega, \theta_0)| = |p_{M-1}(\omega, \theta_0)|, \tag{24}
$$

for $m = 0, \ldots, M-1$, representing different symbols with the same magnitude, such as in PSK-type modulation schemes, then

$$
\frac{|p_0(\omega, \theta_0)|}{N} = \frac{|p_m(\omega, \theta_0)|}{N} = \frac{|p_{M-1}(\omega, \theta_0)|}{N}, \tag{25}
$$

i.e. the magnitudes of coefficients for different antennas and different symbols will become the same. This will further reduce the implementation complexity of the whole DM system.

Now we prove the formulation (20) only works for one desired direction with maximum magnitude response. Without loss of generality, the maximum beam response in the mainlobe direction for one symbol ($m = 0$) is represented by $p_0(\omega, \theta_0) = \frac{\sqrt{2}}{2} + \frac{\sqrt{2}}{2}i$. If there are two desired directions

θ_0 and θ_1 receiving the same symbol, then the equality constraints in (20) can be represented by

$$
w_{0,0}^* + w_{0,1}^* e^{j2\pi d_1 \cos\theta_0} + \ldots + w_{0,N-1}^* e^{j2\pi d_{N-1} \cos\theta_0}
$$
$$
= \frac{\sqrt{2}}{2} + \frac{\sqrt{2}}{2}i
$$
$$
w_{0,0}^* + w_{0,1}^* e^{j2\pi d_1 \cos\theta_1} + \ldots + w_{0,N-1}^* e^{j2\pi d_{N-1} \cos\theta_1}
$$
$$
= \frac{\sqrt{2}}{2} + \frac{\sqrt{2}}{2}i
$$
$$
|w_{0,n}| = \delta_0 = \frac{|p_0(\omega, \theta_0)|}{N} = \frac{1}{N}, \ n = 0, 1, \ldots N-1. \tag{26}
$$

We add up the first two constraints and have the following results

$$
2w_{0,0}^* + w_{0,1}^*(e^{j2\pi d_1 \cos\theta_0} + e^{j2\pi d_1 \cos\theta_1}) + \ldots
$$
$$
+ w_{0,N-1}^*(e^{j2\pi d_{N-1} \cos\theta_0} + e^{j2\pi d_{N-1} \cos\theta_1})
$$
$$
= \sqrt{2} + \sqrt{2}i
$$
$$
\Rightarrow |2w_{0,0}^* + w_{0,1}^*(e^{j2\pi d_1 \cos\theta_0} + e^{j2\pi d_1 \cos\theta_1}) + \ldots
$$
$$
+ w_{0,N-1}^*(e^{j2\pi d_{N-1} \cos\theta_0} + e^{j2\pi d_{N-1} \cos\theta_1})| = 2
$$
$$
\Rightarrow |2w_{0,0}^*| + |w_{0,1}^*(e^{j2\pi d_1 \cos\theta_0} + e^{j2\pi d_1 \cos\theta_1})| + \ldots
$$
$$
+ |w_{0,N-1}^*(e^{j2\pi d_{N-1} \cos\theta_0} + e^{j2\pi d_{N-1} \cos\theta_1})| \geq 2
$$
$$
\Rightarrow 2|w_{0,0}^*| + |w_{0,1}^*| \times |e^{j2\pi d_1 \cos\theta_0} + e^{j2\pi d_1 \cos\theta_1}| + \ldots
$$
$$
+ |w_{0,N-1}^*| \times |e^{j2\pi d_{N-1} \cos\theta_0} + e^{j2\pi d_{N-1} \cos\theta_1}| \geq 2 \tag{27}
$$

When $\theta_0 \neq \theta_1$, we have $|e^{j2\pi d_1 \cos\theta_0} + e^{j2\pi d_1 \cos\theta_1}| < 2$. Then, with $|w_{0,n}| = \frac{|p_0(\omega,\theta_0)|}{N} = \frac{1}{N}$, the left side of the last inequality in (27) can be found to be

$$
\Rightarrow 2|w_{0,0}^*| + |w_{0,1}^*| \times |e^{j2\pi d_1 \cos\theta_0} + e^{j2\pi d_1 \cos\theta_1}| + \ldots
$$
$$
+ |w_{0,N-1}^*| \times |e^{j2\pi d_{N-1} \cos\theta_0} + e^{j2\pi d_{N-1} \cos\theta_1}|
$$
$$
< \frac{1}{N} \times 2 + \frac{1}{N} \times 2 + \ldots + \frac{1}{N} \times 2 = 2, \tag{28}
$$

However, according to (27), it should be larger or equal to 2, which contradicts the above result. As a result, the number of directions with the same maximum magnitude value cannot be larger than one.

For eavesdroppers with a known direction, we can apply a corresponding constraint to make the beam response at this direction as low as possible. This constraint will not affect the proposed constant magnitude constraint.

Another note is that the proposed constraint cannot only be applied to a linear antenna array, but also a planar antenna array or a circular antenna array by changing the corresponding steering vectors.

IV. DESIGN EXAMPLES

In this section, we consider an $N = 20$ ULA with a half wavelength spacing between adjacent antennas. Note that the proposed constraint works well irrespective of the number of antennas. Both broadside and off-broadside designs are provided. For the broadside design, the desired direction is pointed to $\theta_{ML} = 90°$, while $\theta_{SL} \in [0°, 85°] \cup [95°, 180°]$ for
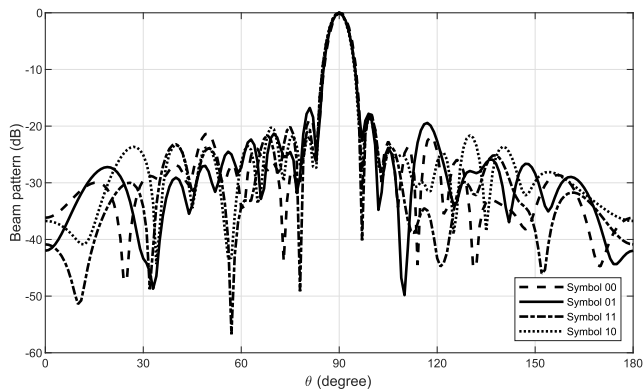
FIGURE 2. Resultant beam responses for the broadside design without magnitude constraint in (8).
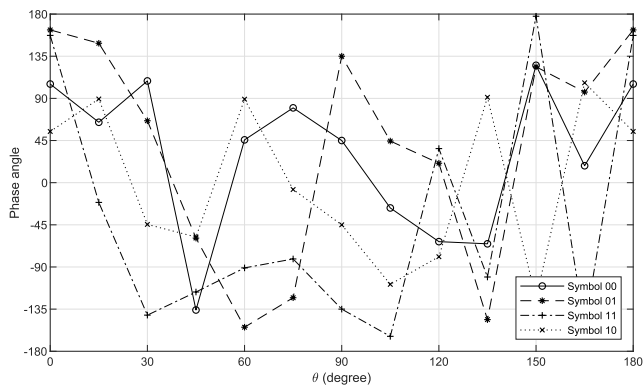

FIGURE 3. Resultant phase responses for the broadside design without magnitude constraint in (8).

the sidelobe region. For the off-broadside design, $\theta_{ML} = 60°$ and $\theta_{SL} \in [0°, 55°] \cup [65°, 180°]$. The desired response in the desired direction is a value of one (magnitude) with $90°$ phase shift (QPSK), i.e.,

$$\frac{\sqrt{2}}{2} + i\frac{\sqrt{2}}{2}, -\frac{\sqrt{2}}{2} + i\frac{\sqrt{2}}{2}, -\frac{\sqrt{2}}{2} - i\frac{\sqrt{2}}{2}, \frac{\sqrt{2}}{2} - i\frac{\sqrt{2}}{2} \quad (29)$$

for symbols '00', '01', '11', '10', and a value of 0.1 (magnitude) with random phase shifts over the sidelobe regions. The constant magnitude of weight coefficient

$$\frac{|p_m(\omega, \theta_0)|}{N} = 0.05. \quad (30)$$

To verify the performance of the proposed design, the beam and phase patterns for the designs with and without constant magnitude constraint for weight coefficients are given. Bit error rate (BER) is calculated based on which quadrant the received complex-valued signal falls into. Here the signal to noise ratio (SNR) is set at 12 dB in the mainlobe direction, 10^6 bits are transmitted, and the same additive white Gaussian noise (AWGN) power levels for all directions are also assumed.

For the broadside design without constant magnitude constraint in (8), Figs. 2 and 3 show the beam and phase patterns for symbols '00, 01, 11, 10', where we can see that all main beams are exactly pointed to $90°$ (the desired direction)

TABLE 2. Magnitude of weight coefficients for the broadside design without magnitude constraint in (8) for symbol '00' ($m = 0$).

Weight	Magnitude	Weight	Magnitude	Weight	Magnitude
$w_{m,0}$	0.0306	$w_{m,7}$	0.0623	$w_{m,14}$	0.0556
$w_{m,1}$	0.0372	$w_{m,8}$	0.0593	$w_{m,15}$	0.0573
$w_{m,2}$	0.0309	$w_{m,9}$	0.0630	$w_{m,16}$	0.0489
$w_{m,3}$	0.0338	$w_{m,10}$	0.0693	$w_{m,17}$	0.0457
$w_{m,4}$	0.0551	$w_{m,11}$	0.0588	$w_{m,18}$	0.0395
$w_{m,5}$	0.0582	$w_{m,12}$	0.0602	$w_{m,19}$	0.0223
$w_{m,6}$	0.0584	$w_{m,13}$	0.0637		

TABLE 3. Magnitude of weight coefficients for the broadside design without magnitude constraint in (8) for symbol '01' ($m = 1$).

Weight	Magnitude	Weight	Magnitude	Weight	Magnitude
$w_{m,0}$	0.0310	$w_{m,7}$	0.0539	$w_{m,14}$	0.0480
$w_{m,1}$	0.0359	$w_{m,8}$	0.0600	$w_{m,15}$	0.0426
$w_{m,2}$	0.0423	$w_{m,9}$	0.0688	$w_{m,16}$	0.0450
$w_{m,3}$	0.0407	$w_{m,10}$	0.0661	$w_{m,17}$	0.0405
$w_{m,4}$	0.0631	$w_{m,11}$	0.0565	$w_{m,18}$	0.0337
$w_{m,5}$	0.0741	$w_{m,12}$	0.0489	$w_{m,19}$	0.0305
$w_{m,6}$	0.0665	$w_{m,13}$	0.0577		

TABLE 4. Magnitude of weight coefficients for the broadside design without magnitude constraint in (8) for symbol '11' ($m = 2$).

Weight	Magnitude	Weight	Magnitude	Weight	Magnitude
$w_{m,0}$	0.0316	$w_{m,7}$	0.0642	$w_{m,14}$	0.0551
$w_{m,1}$	0.0308	$w_{m,8}$	0.0712	$w_{m,15}$	0.0512
$w_{m,2}$	0.0423	$w_{m,9}$	0.0687	$w_{m,16}$	0.0537
$w_{m,3}$	0.0550	$w_{m,10}$	0.0612	$w_{m,17}$	0.0372
$w_{m,4}$	0.0389	$w_{m,11}$	0.0623	$w_{m,18}$	0.0258
$w_{m,5}$	0.0510	$w_{m,12}$	0.0582	$w_{m,19}$	0.0148
$w_{m,6}$	0.0663	$w_{m,13}$	0.0652		

TABLE 5. Magnitude of weight coefficients for the broadside design without magnitude constraint in (8) for symbol '10' ($m = 3$).

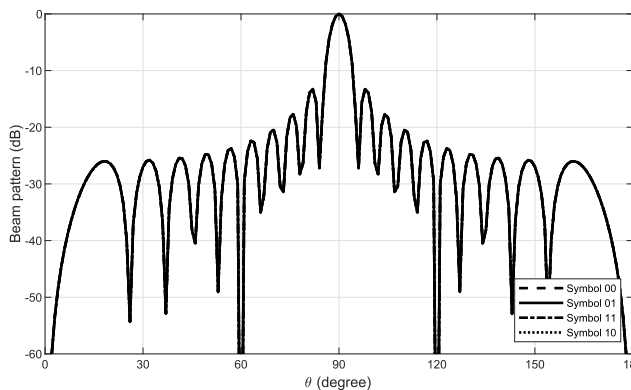| Weight	Magnitude	Weight	Magnitude	Weight	Magnitude
$w_{m,0}$	0.0358	$w_{m,7}$	0.0666	$w_{m,14}$	0.0522
$w_{m,1}$	0.0438	$w_{m,8}$	0.0684	$w_{m,15}$	0.0420
$w_{m,2}$	0.0394	$w_{m,9}$	0.0684	$w_{m,16}$	0.0502
$w_{m,3}$	0.0516	$w_{m,10}$	0.0608	$w_{m,17}$	0.0288
$w_{m,4}$	0.0407	$w_{m,11}$	0.0572	$w_{m,18}$	0.0340
$w_{m,5}$	0.0626	$w_{m,12}$	0.0595	$w_{m,19}$	0.0235
$w_{m,6}$	0.0632	$w_{m,13}$	0.0643		

FIGURE 4. Resultant beam responses for the broadside design with magnitude constraint in (23).

with a low sidelobe level, and the phases in the desired direction follow the standard QPSK constellation mappings, but random for the rest of the angles. However, as shown in Tables 2, 3, 4 and 5, the magnitude of weight coefficients
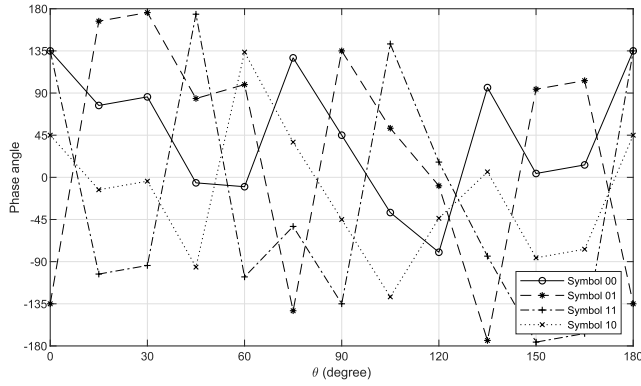
FIGURE 5. Resultant phase responses for the broadside design with magnitude constraint in (23).

TABLE 6. Magnitude of weight coefficients for both broadside and off-broadside designs with magnitude constraint in (23) for symbols '00', '01', '11' and '10' ($m = 0, 1, 2, 3$).

Weight	Magnitude	Weight	Magnitude	Weight	Magnitude
$w_{m,0}$	0.05	$w_{m,7}$	0.05	$w_{m,14}$	0.05
$w_{m,1}$	0.05	$w_{m,8}$	0.05	$w_{m,15}$	0.05
$w_{m,2}$	0.05	$w_{m,9}$	0.05	$w_{m,16}$	0.05
$w_{m,3}$	0.05	$w_{m,10}$	0.05	$w_{m,17}$	0.05
$w_{m,4}$	0.05	$w_{m,11}$	0.05	$w_{m,18}$	0.05
$w_{m,5}$	0.05	$w_{m,12}$	0.05	$w_{m,19}$	0.05
$w_{m,6}$	0.05	$w_{m,13}$	0.05		

FIGURE 6. BER for the broadside design with magnitude constraint in (23).

FIGURE 7. Resultant beam responses for the off-broadside design with magnitude constraint in (23).

FIGURE 8. Resultant phase responses for the off-broadside design with magnitude constraint in (23).
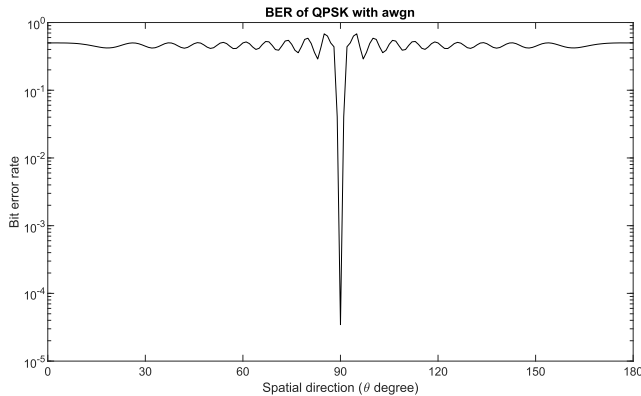

FIGURE 9. BER for the off-broadside design with magnitude constraint in (23).

are not the same; in other words, constant magnitude for weight coefficients are not achieved.

In contrast, for the design with constant magnitude constraint in (23), Figs. 4 and 5 show the corresponding beam and phase patterns, which satisfies the DM design. The magnitudes of all weight coefficients are shown in Table 6. It can be seen that all magnitudes are equal to 0.05, the same as the given magnitude $\frac{|p_m(\omega,\theta_0)|}{N} = 0.5$, demonstrating the effectiveness of the proposed design. The BER performance of the proposed design is shown in Fig. 6, where we can see that in 90° (the desired direction) the value is down to 10^{-5}, while at other directions it fluctuates around 0.5, illustrating the practicality of the proposed design.

For the off-broadside design with constant magnitude constraint in (23), Figs. 7 and 8 show the corresponding beam
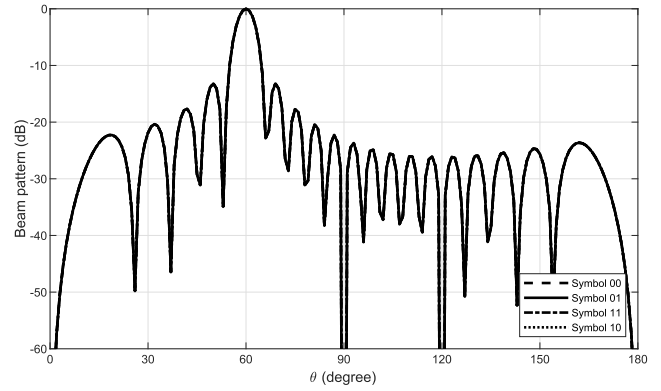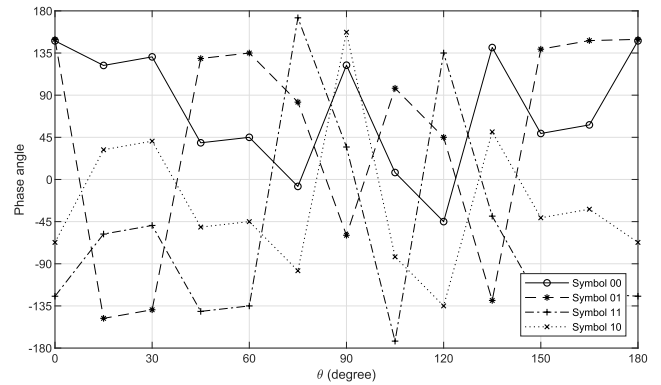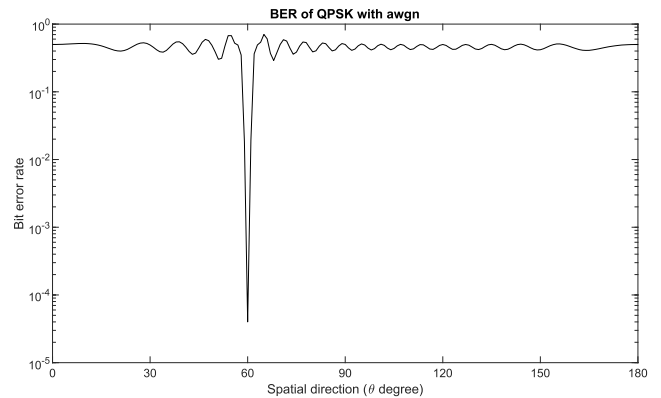
and phase patterns, where we can see that the main beam points to the desired direction 60°, with a standard QPSK. The magnitudes of all weight coefficients are the same as 0.05, as shown in Table 6. The corresponding BER performance is shown in Fig. 9, again with a satisfactory result.

V. CONCLUSION
To reduce the implementation complexity, a constant magnitude constraint for weight coefficients has been introduced into the directional modulation design for the first time, and

by employing the absolute value inequalities, the resultant non-convex constant magnitude constraint is transformed into a convex form so that its solution can be found conveniently by existing convex optimisation toolboxes. As shown in the provided design examples, with the proposed constraint, a constant magnitude of weight coefficients can be achieved for different antennas with a given symbol, and when all the magnitudes of the symbols are the same, we will have a constant weight coefficient magnitude for all antennas and symbols, with an even lower implementation complexity.

REFERENCES

[1] X. Liu, M. Jia, X. Zhang, and W. Lu, "A novel multichannel Internet of Things based on dynamic spectrum sharing in 5G communication," *IEEE Internet Things J.*, vol. 6, no. 4, pp. 5962–5970, Aug. 2019.

[2] X. Liu and X. Zhang, "Rate and energy efficiency improvements for 5G-based IoT with simultaneous transfer," *IEEE Internet Things J.*, vol. 6, no. 4, pp. 5971–5980, Aug. 2019.

[3] A. Babakhani, D. B. Rutledge, and A. Hajimiri, "Near-field direct antenna modulation," *IEEE Microw. Mag.*, vol. 10, no. 1, pp. 36–46, Feb. 2009.

[4] M. P. Daly and J. T. Bernhard, "Beamsteering in pattern reconfigurable arrays using directional modulation," *IEEE Trans. Antennas Propag.*, vol. 58, no. 7, pp. 2259–2265, Jul. 2010.

[5] M. P. Daly and J. T. Bernhard, "Directional modulation technique for phased arrays," *IEEE Trans. Antennas Propag.*, vol. 57, no. 9, pp. 2633–2640, Sep. 2009.

[6] B. Zhang, W. Liu, and X. Gou, "Compressive sensing based sparse antenna array design for directional modulation," *IET Microw., Antennas Propag.*, vol. 11, no. 5, pp. 634–641, Apr. 2017.

[7] B. Zhang and W. Liu, "Antenna array based positional modulation with a two-ray multi-path model," in *Proc. IEEE 10th Sensor Array Multichannel Signal Process. Workshop (SAM)*, Sheffield, U.K., Jul. 2018, pp. 203–207.

[8] B. Zhang and W. Liu, "Positional modulation design based on multiple phased antenna arrays," *IEEE Access*, vol. 7, pp. 33898–33905, 2019.

[9] B. Zhang, W. Liu, and X. Lan, "Orthogonally polarized dual-channel directional modulation based on crossed-dipole arrays," *IEEE Access*, vol. 7, pp. 34198–34206, 2019.

[10] B. Zhang and W. Liu, "Multi-carrier based phased antenna array design for directional modulation," *IET Microw., Antennas Propag.*, vol. 12, no. 5, pp. 765–772, Apr. 2018.

[11] B. Zhang, W. Liu, and Q. Li, "Multi-carrier waveform design for directional modulation under peak to average power ratio constraint," *IEEE Access*, vol. 7, pp. 37528–37535, 2019.

[12] T. Hong, M.-Z. Song, and Y. Liu, "Dual-beam directional modulation technique for physical-layer secure communication," *IEEE Antennas Wireless Propag. Lett.*, vol. 10, pp. 1417–1420, 2011.

[13] H. Shi and A. Tennant, "Enhancing the security of communication via directly modulated antenna arrays," *IET Microw., Antennas Propag.*, vol. 7, no. 8, pp. 606–611, Jun. 2013.

[14] Y. Ding and V. Fusco, "Directional modulation transmitter synthesis using particle swarm optimization," in *Proc. Loughborough Antennas Propag. Conf.*, Loughborough, U.K., Nov. 2013, pp. 500–503.

[15] Y. Ding and V. Fusco, "Directional modulation transmitter radiation pattern considerations," *IET Microw., Antennas Propag.*, vol. 7, no. 15, pp. 1201–1206, Dec. 2013.

[16] Y. Ding and V. F. Fusco, "Directional modulation far-field pattern separation synthesis approach," *IET Microw., Antennas Propag.*, vol. 9, no. 1, pp. 41–48, 2015.

[17] Q. Zhu, S. Yang, R. Yao, and Z. Nie, "Directional modulation based on 4-D antenna arrays," *IEEE Trans. Antennas Propag.*, vol. 62, no. 2, pp. 621–628, Feb. 2014.

[18] T. Xie, J. Zhu, and Y. Li, "Artificial-noise-aided zero-forcing synthesis approach for secure multi-beam directional modulation," *IEEE Commun. Lett.*, vol. 22, no. 2, pp. 276–279, Feb. 2018.

[19] W. Zhu, F. Shu, T. Liu, X. Zhou, J. Hu, G. Liu, L. Gui, J. Li, and J. Lu, "Secure precise transmission with multi-relay-aided directional modulation," in *Proc. 9th Int. Conf. Wireless Commun. Signal Process. (WCSP)*, Oct. 2017, pp. 1–5.

[20] Y. Ding and V. F. Fusco, "A vector approach for the analysis and synthesis of directional modulation transmitters," *IEEE Trans. Antennas Propag.*, vol. 62, no. 1, pp. 361–370, Jan. 2014.

[21] Y. Ding and V. F. Fusco, "Vector representation of directional modulation transmitters," in *Proc. 8th Eur. Conf. Antennas Propag. (EuCAP)*, Apr. 2014, pp. 367–371.

[22] J. S. Hu, F. Shu, and J. Li, "Robust synthesis method for secure directional modulation with imperfect direction angle," *IEEE Commun. Lett.*, vol. 20, no. 6, pp. 1084–1087, Jun. 2016.

[23] J. Hu, S. Yan, F. Shu, J. Wang, J. Li, and Y. Zhang, "Artificial-noise-aided secure transmission with directional modulation based on random frequency diverse arrays," *IEEE Access*, vol. 5, pp. 1658–1667, 2017.

[24] M. Grant and S. Boyd, "Graph implementations for nonsmooth convex programs," in *Recent Advances in Learning and Control* (Lecture Notes in Control and Information Sciences), V. Blondel, S. Boyd, and H. Kimura, Eds. London, U.K.: Springer-Verlag, 2008, pp. 95–110. [Online]. Available: http://stanford.edu/~boyd/graph_dcp.html

[25] Centaur Research. (Sep. 2012). *CVX: MATLAB Software for Disciplined Convex Programming, Version 2.0 Beta*. [Online]. Available: http://cvxr.com/cvx

BO ZHANG received the B.Sc. degree from Tianjin Normal University, China, in 2011, and the M.Sc. and Ph.D. degrees from the Department of Electrical and Electronic Engineering, The University of Sheffield, in 2013 and 2018, respectively.

He is currently with the College of Electronic and Communication Engineering, Tianjin Normal University. His research interests include array signal processing (beamforming and direction of arrival estimation and so on.), directional modulation, and sparse array design.
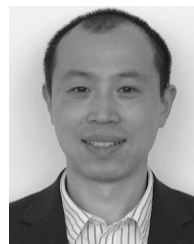
WEI LIU (S'01–M'04–SM'10) received the B.Sc. and LLB degrees from Peking University, China, in 1996 and 1997, respectively, the M.Phil. degree from The University of Hong Kong, in 2001, and the Ph.D. degree from the School of Electronics and Computer Science, University of Southampton, U.K., in 2003.

He held a postdoctoral position first at Southampton and later at the Department of Electrical and Electronic Engineering, Imperial College London. Since September 2005, he has been with the Department of Electronic and Electrical Engineering, The University of Sheffield, U.K., first as a Lecturer and then a Senior Lecturer. He has published more than 300 journal and conference papers, five book chapters, and two research monographs titled *Wideband Beamforming: Concepts and Techniques* (John Wiley, March 2010), *Low-Cost Smart Antennas* (Wiley-IEEE, March 2019), and *Low-Cost Smart Antennas* (Wiley-IEEE, March 2019). His research interests include wide range of topics in signal processing, with a focus on sensor array signal processing and its various applications, such as robotics and autonomous vehicles, human–computer interface, big data analytics, radar, sonar, satellite navigation, and wireless communications. He is currently a member of the Digital Signal Processing Technical Committee, the IEEE Circuits and Systems Society and the Sensor Array and Multichannel Signal Processing Technical Committee, the IEEE Signal Processing Society (Vice-Chair from January 2019). He was an Associate Editor of the IEEE TRANSACTIONS ON SIGNAL PROCESSING, from 2015 to 2019. He is also an Associate Editor of IEEE ACCESS and an Editorial Board Member of the *Journal Frontiers of Information Technology and Electronic Engineering*.

YANG LI received the B.E. and M.E. degrees from the College of Information Technology and Science, Nankai University, Tianjin, in 2008 and 2012, respectively, and the Ph.D. degree from the Department of Engineering, Tohoku University, Sendai, in 2017. He is currently with the College of Electronic and Communication Engineering, Tianjin Normal University. His research interests include antenna design, EM-wave propagation, and sensor networks.

XIAONAN ZHAO received the Ph.D. degree from Tianjin University, Tianjin, in 2015. He is currently with the College of Electronic and Communication Engineering, Tianjin Normal University. His research interest includes wireless communication channel measurement and modeling.

CHENG WANG received the B.E. degree in measurement and control technology from Xidian University, Xi'an, China, in 2006, and the M.E. and Ph.D. degrees in communication engineering and electrical engineering from Nankai University, Tianjin, China, in 2010 and 2014, respectively.

From 2012 to 2014, the China Scholarship Council sent him to Columbia University, New York, USA, as a Joint Training Doctoral Scholar. During the visiting study, he switched his research interests into condensed matter physics and nanoelectronics. He was an Interdisciplinary Postdoctoral Research with Tsinghua University, Beijing, China, from 2015 to 2017, after then, he joined Tianjin Normal University, in 2017, as a Principal Investigator directing the Interdisciplinary Laboratory of Advanced Materials and Devices (X-Lab). His current research interest includes 2-D nanomaterials and devices.

• • •